

2-25-2008

Determination of the Eigenstates and Wavefunctions of a Single Gated As Donor

Gabriel P. Lansbergen

Kavli Institute of Nanoscience, Delft University of Technology

R. Rahman

Network for Computational Nanotechnology, Purdue University

C. J. Wellard

University of Melbourne

P. E. Rutten

Kavli Institute of Nanoscience, Delft University of Technology

J. Caro

Kavli Institute of Nanoscience, Delft University of Technology

See next page for additional authors

Follow this and additional works at: <http://docs.lib.purdue.edu/nanodocs>

 Part of the [Nanoscience and Nanotechnology Commons](#)

Lansbergen, Gabriel P.; Rahman, R.; Wellard, C. J.; Rutten, P. E.; Caro, J.; Woo, I.; Colleart, N.; Biersemans, S.; and Klimeck, Gerhard, "Determination of the Eigenstates and Wavefunctions of a Single Gated As Donor" (2008). *Other Nanotechnology Publications*. Paper 155.

<http://docs.lib.purdue.edu/nanodocs/155>

This document has been made available through Purdue e-Pubs, a service of the Purdue University Libraries. Please contact epubs@purdue.edu for additional information.

Authors

Gabriel P. Lansbergen, R. Rahman, C. J. Wellard, P. E. Rutten, J. Caro, I. Woo, N. Colleart, S. Biersemans, and Gerhard Klimeck

Determination of the eigenstates and wavefunctions of a single gated As donor

G.P.Lansbergen¹, R. Rahman², C.J. Wellard³, P.E. Ruten¹, J. Caro¹, I. Woo², N. Colleart⁴,
S. Biesemans⁴, G. Klimeck^{2,5}, L.C.L. Hollenberg³, S. Rogge¹

¹ Kavli Institute of Nanoscience, Delft University of Technology, Lorentzweg 1, 2628 CJ Delft, The Netherlands

² Network for Computational Nanotechnology, Purdue University, West Lafayette, Indiana 47907, USA

³ The Center for Quantum Computer Technology, School of Physics, University of Melbourne, VIC 3010, Australia

⁴ InterUniversity Microelectronics Center (IMEC), Kapeldreef 75, 3001 Leuven, Belgium

⁵ Jet Propulsion Laboratory, California Institute of Technology, Pasadena, California 91109, USA

Abstract— Current semiconductor devices have been scaled to such dimensions that we need take atomistic approach to understand their operation for nano-electronics. From a bottom-up perspective, the smallest functional element within a nano-device would be a single (dopant) atom itself. Control and understanding over the eigenenergies and wavefunctions of a single dopant could prove a key ingredient for device technology beyond-CMOS. Here, we will discuss the eigenlevels of a single As donor in a three terminal configuration. The donor is incorporated in the channel of prototype transistors called FinFETs. The measured eigenlevels are shown to consist of levels associated with the donors Coulomb potential, levels associated with a triangular well at the gate interface and hybridized combinations of the two. The theoretical framework in which we describe this system (NEMO-3D) is based on a tight-binding approximation.

Keywords; Single donor, Resonant tunneling spectroscopy;

I. INTRODUCTION

Isolated donors in silicon have received renewed attention in the last decade due to their potential use in quantum electronics [1-6]. The donors form 3D Coulomb (thus truly atomistic) potentials in the silicon lattice that can bind up to two electrons [7]. In the majority of proposals for silicon quantum electronics, isolated donors act as the binding sites for the information-carrying electrons. The ability to perform (quantum) operations is crucially provided by one (or more) gate electrodes around the donor site. Although many proposals are based on the functionality of isolated single donors, experimental access to such systems is difficult (but has been successfully achieved in a few occasions [8-10].)

Here, we will discuss resonant tunneling spectroscopy measurements on the eigenlevels of single As donors in a three terminal configuration, i.e. a gated donor which is a basic element for quantum electronics. The donors are incorporated in the channel of (p-type) prototype transistors called FinFETs. The local electric field due to the built-in voltage between the channel and the gate electrode forms a triangular potential at the interface. We will show that by means of spectroscopic measurements we can identify states to be associated with

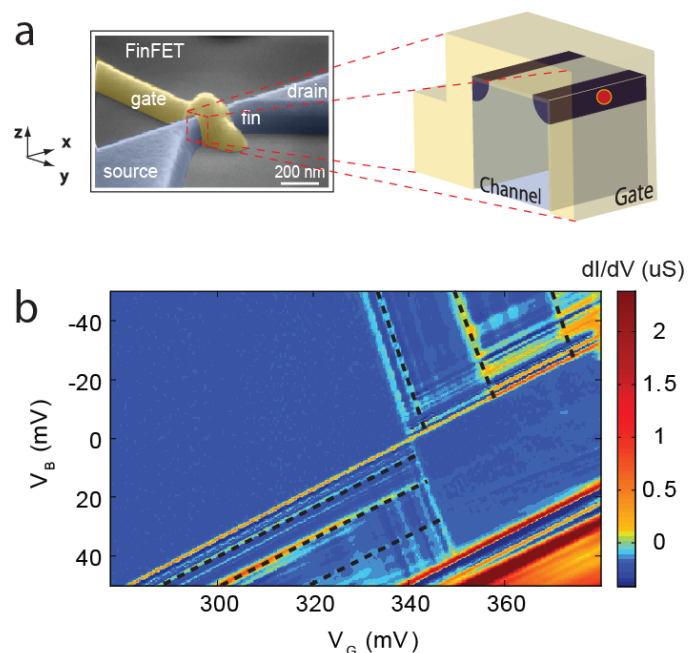


Figure 1. a) Colored Scanning Electron Micrograph of a FinFET device. Blow-up schematically shows channel/gate with current-carrying region (dark-blue) and donor atom (red dot). b) Stability diagram of a typical D^0 charge state. The dashed black lines indicate the presence of excited eigenlevels.

either the donors Coulomb potential, the triangular well or a hybridized combinations of the two. The theoretical framework used to describe this system is based on a tight binding approximation. The correspondence between the transport measurements, the theoretical model and the local environment of the donor provides a robust atomic understanding of actual gated donors.

II. FINFET DEVICE STRUCTURE

The FinFETs consist of crystalline silicon wires (fins) with large contacts patterned by 193 nm optical lithography and dry

etching from Silicon-On-Insulator. After a boron channel implantation, a 100 nm polycrystalline silicon was deposited on top of a nitrided oxide (1.4 nm equivalent SiO₂ oxide thickness), then received a phosphorus (P) implant as predoping, and was patterned using an oxide hard mask to form a narrow gate. Next, we used high-angle arsenic (As) implantations as source or drain extensions, while the channel was protected by the gate and 50 nm wide nitride spacers and remains p type. Finally, As and P implants and a NiSi metallic silicide are used to complete the source or drain electrodes. The samples in this research have a gate length of 60 nm. Due to the relatively increased capacitance between the gate electrode and the corner regions of the nanowire, the later experiences a reduced potential. This so-called corner effect confines the source/drain-current to a narrow region at the very edges [11] which contains only a few As donor atoms. These donors originate most probably from transient enhanced diffusion at the Si/SiO₂ interface [12] out of the As source/drain contact extensions. In about one out of seven devices the distinctive resonances of the D⁰ and D⁻ charge states of a single As donor can be observed in the transport measurements [9]. Note that we do not control the position of the donors in the channel and rely on statistical change for a donor to be present in the corner regions of the channel. Since we know the donors to be located in the corner regions they are also necessarily close to the gate interface.

III. EIGENSTATES OF A SINGLE GATED DONOR

In this work, we will mainly focus on the eigenlevels of the D⁰ (single electron) charge state. These eigenlevels are determined from its measured stability diagram, i.e. a plot of the differential source/drain conductance (dI/dV) as a function of bias voltage (V_B) and gate voltage (V_G), see Fig. 1b. At $V_B = 0$, the D⁰ state is at resonance with the source/drain contacts at a gate voltage of 340 mV. Here, the charge fluctuates between 0 and 1 electron. The total electric transport increases as an excited eigenlevel of the one-electron state (D⁰) enters the bias window defined by source/drain, giving the stability diagram its characteristic pattern [12] indicated by the dashed black lines. The red dots indicate the combinations of V_B and V_G where the ground state is at the Fermi energy of the drain and an excited state is at the Fermi energy of the source. It is the bias voltage V_B in this combination that is a direct measure for the eigenergy of the excited state ($e V_{B,N} = E_N$), where E_N is the energy relative to the ground state and N is a label for the level). The excited states as determined in this fashion are depicted in Table I (in the appendix).

The measured level spectrum does not match the level spectrum of a bulk donor, but are heavily influenced by the electric field from the nearby gate electrode [13]. The electric field is induced by the built-in voltage between gate and channel and can be estimated to be at around 21 MV/m. This estimation is based on a numerical solution of the Poisson equation and the charge distribution in a corner geometry. This is quite comparable to the Bohr field of the donor, ~ 30 MV/m.

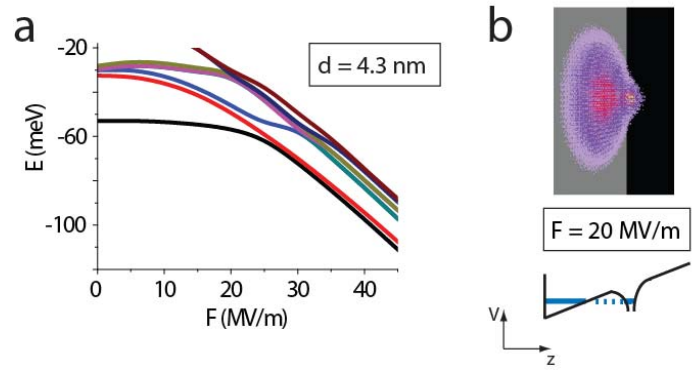


Figure 2. a) Eigenenergies (E) of an As donor 4.3 nm below a SiO₂ interface as a function of electric field (F) calculated in a tight-binding approximation. b) Wavefunction density of the ground state of an As donor at $d = 4.3$ nm and $F = 20$ MV/m. The gray plane represents the SiO₂ interface. The ground state is a hybrid combination of donor-like and well-like states.

The eigenlevels of a gated As donor were calculated in an atomistic multi-million atom tight-binding approximation (NEMO 3-D) as both a function of local electric field (F) and distance to the gate interface (d). The corners of the FinFET are actually rounded with a radius of about 5 nm (about two times the Bohr radius of a bulk As donor) and thus justifies the planar nature of this model. (Screening effects are not taken into account here, which will be discussed later on.) Figure 2a shows the eigenenergies as a function of field for $d = 4.3$ nm as an example.

Three electric field regimes can be distinguished. At the low field limit ($F \sim 0$ mV/m) we obtain the spectrum of a bulk As donor. In the high field limit ($F \sim 40$ MV/m) the electron is pulled into the triangular well at the interface and the donor is ionized. In the cross-over regime ($F \sim 20$ MV/m) the electron is delocalized over the donor- and triangular well potential. Strong tunneling interaction between the two sites causes hybridization of levels characterized by the anti-crossing behavior of spectral lines. The ground state is a hybridized anti-bonding state of well-like and donor-like parts, see Fig. 2b.

The first three measured excited states of the D⁰ state were fitted into the calculated spectrum with F and d as the two (independent) degrees of freedom. The six measured samples can be fit within the theoretical data with a standard deviation of about 0.5 meV, see Table I. This is to be interpreted as an estimated error of about 0.5 meV *per* excited level (due to the two extra degrees of freedom of the fit), which is in line with the measurement error we expect from the analysis of the stability diagrams.

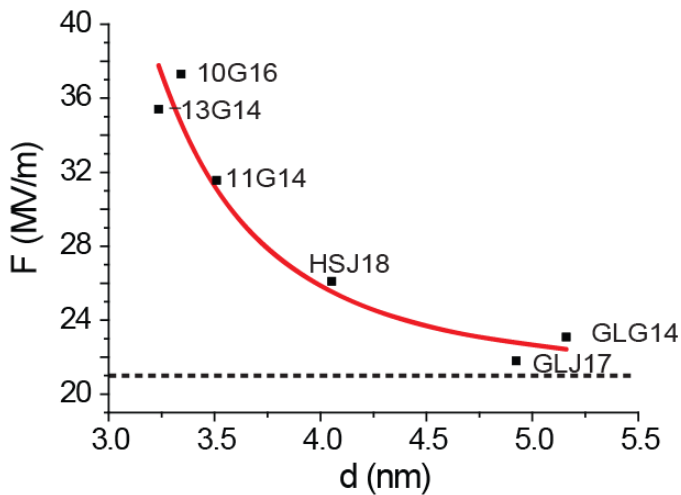


Figure 3. Local electric field F versus donor depth d as predicted by the tight-binding model. The labels represent the corresponding devices. The F as expected from electrostatic modeling of the FinFET devices is indicated by the dashed line. The red curve is a fit of the data to a classical model of the interface screening as described in the text.

IV. LOCAL DONOR ENVIRONMENT

The local electric field (F) and donor depth (d) for each donor that follows from the tight-binding fit can be separately compared to independent determinations of their local environments. The charging energy of the D^- charge state is a direct measure of the donors distance to the gate interface (d). It follows from top of the Coulomb diamond between the D^0 and D^- as indicated in Fig 1b, as shown for all six samples in Table I. The fact that the charging energy of the donors is reduced shows the donors are subjected to a (attractive) metallic screening. And, as can be readily observed, donors that are predicted to be closer to the interface by the TB-fit have a smaller charging energy. We explain the metallic behavior by the majority of Arsenic donors in the channel preferentially being segregated at the Si/SiO₂ interface [15], where it forms a (dipole) screening layer [14]. We can make a rough estimate of the reduction of the charging energy as a function of the donors distance to the interface by simply considering the donor as a small sphere which capacitance is reduced by the proximity of a metallic plate (the interface). This yields a surprisingly good result, see Table I.

The local electric field consists of the electric field due to the built-in voltage and a contribution from the screening of the donor's dipole moment again by the gate interface. Figure 3 shows the positions of the measured donors in the F versus d plane as determined from the tight-binding fit. We find a trend for donors close to the interface to experience a higher local electric field, see Fig. 3, which can also be related to the aforementioned metallic-like screening at the Si/SiO₂ interface. The red curve shows a fit of the data-points assuming the donor nucleus and electron as point charges with a dipole arm a separating the two. This toy-model yields a very realistic dipole arm of $a = 2.1$ nm and captures the magnitude of the effect

well, supporting our ideas on the metallic screening behavior of the interface.

Although the screening can be classified as attractive, we are unable to quantify the exact amount of screening that each donor is subjected to. However, we can show that the results of Figure 3 do not show any significant change if we assume a attractive screening interface in the (fully self-consistent) tight-binding fit (up to the strength of about half that of being a full metal.)

V. CONCLUSIONS

We have performed transport measurement through single donors in a nanostructure and observe directly the action of a gate electrode on their energy levels. The correspondence we find between the measured eigenlevels in the six samples and a multi-million tight-binding approximation shows we have a robust model for As donor states in a silicon three-terminal geometry. Furthermore, the model is able to predict the (independently determined) local environment of each donor, giving us confidence that we have an accurate description of a real gated donor in a nanostructure.

REFERENCES

- [1] B.E. Kane, "A silicon-based nuclear spin quantum computer", *Nature* 393, 133 (1998).
- [2] R. Vrijen et al., "Electron-spin-resonance transistors for quantum computing in silicon-germanium heterostructures", *Phys. Rev. A* 62, 012306 (2000).
- [3] F. Ruess et al., "Realization of Atomically Controlled Dopant Devices in Silicon", *Small* 3, 563 (2007)
- [4] L.C.L. Hollenberg et al., "Charge-based quantum computing using single donors in semiconductors", *Phys. Rev B* 69, 113301 (2004)
- [5] L.C.L. Hollenberg, A.D. Greentree, A.G. Fowler and C.J. Wellard, "Two-dimensional architectures for donor-based quantum computing", *Phys. Rev B* 74, 045311 (2006)
- [6] R. de Sousa, J.D. Delgado and S. Das Sarma, "Silicon quantum computation based on magnetic dipolar coupling", *Phys. Rev. A* 70, 052304 (2004)
- [7] This holds for shallow donors, see M. Taniguchi and S. Narita, " D^- state in silicon", *Solid State Commun.* 20, 131 (1976)
- [8] L.E. Calvet, R.G. Wheeler and M.A. Reed, "Observation of the Linear Stark Effect in a Single Acceptor in Si", *Phys. Rev. Lett.* 98, 096805 (2007)
- [9] H. Sellier et al., "Transport Spectroscopy of a Single Dopant in a Gated Silicon Nanowire", *Phys. Rev. Lett.* 97, 206805 (2006)
- [10] S.E.S. Andresen et al., "Charge state control and relaxation in an atomically doped silicon device", *Nano Lett.* 7, 2000 (2007)
- [11] H. Sellier et al., "Subthreshold channels at the edges of nanoscale triple-gate silicon transistors", *Appl. Phys. Lett.* 90, 073502 (2007)
- [12] L.P. Kouwenhoven et al., in *Mesoscopic Electron Transport*, edited by L. L. Sohn, L. P. Kouwenhoven, and G. Schön (Kluwer, Dordrecht, 1997).
- [13] M.J. Calderón, B. Koiler, X. Hu., S. Das Sarma, "Quantum Control of Donor Electrons at the Si/SiO₂ Interface, *Phys. Rev. Lett.* 96, 096802 (2006)
- [14] Z. Zhou et al., "Dopant local bonding and electrical activity near Si(001)-oxide interfaces", *J. Appl. Phys.* 98, 076105 (2005)
- [15] R. Kasnavi et al., "Characterization of arsenic dose loss at the Si/SiO₂ interface", *J. Appl. Phys.* 87, 2255 (2000).

VI. APPENDIX A

TABLE I. FIRST THREE MEASURED EXCITED STATES OF EACH SAMPLE VERSUS THE BEST FIT TO A TIGHTBINDING MODEL. ALSO GIVEN ARE THE DONOR DEPTHS (UNDER THE Si/SiO₂ INTERFACE) THAT WERE OBTAINED FROM THE MEASURED CHARGING ENERGY VERSUS THE DISTANCE OBTAINED FROM THE TB-FIT. THE RIGHT-MOST COLUMN OF THE TABLE LISTS THE PREDICTIONS FOR THE LOCAL ELECTRIC FIELD AND THE (SAMPLE SPECIFIC) STANDARD DEVIATION OF THE FIT S.

Device		E1 (meV)	E2 (meV)	E3 (meV)	E _c (meV)	d (nm)	F (MV m ⁻¹)	S (meV)
<i>10G16</i>	<i>Exp.</i>	2	15	23	30	3.3		
	<i>T.B.</i>	2.2	15.6	23.0	-	3.3	37.3	0.59
<i>11G14</i>	<i>Exp.</i>	4.5	13.5	25	29	3.2		
	<i>T.B.</i>	4.5	13.5	25.0	-	3.5	31.6	0.04
<i>13G14</i>	<i>Exp.</i>	3.5	15.5	26.4	29	3.2		
	<i>T.B.</i>	3.6	15.7	26.3	-	3.2	35.4	0.17
<i>HSJ18</i>	<i>Exp.</i>	5	10	21.5	33	4.0		
	<i>T.B.</i>	4.5	9.9	21.8	-	4.1	26.1	0.63
<i>GLG14</i>	<i>Exp.</i>	1.3	10	13.2	35	4.7		
	<i>T.B.</i>	1.3	10	12.4	-	5.2	23.1	0.28
<i>GLJ17</i>	<i>Exp.</i>	2	7.7	15.5	33	4.0		
	<i>T.B.</i>	1.3	7.7	15.8	-	4.9	21.9	0.77